Preprints (www.preprints.org) | NOT PEER-REVIEWED | Posted: 22 June 2018 doi:10.20944/preprints201806.0346.v1

Peer-reviewed version available at *Energies* **2018**, *11*, 1810; doi:10.3390/en11071810

Article

Online State of Charge and State of Health Estimation for Lithium-Ion Battery Based on a Data-Model Fusion Method

Zhongbao Wei [1,*], Feng Leng [1], Zhongjie He [1], Wenyu Zhang [1], and Kaiyuan Li [1]

[1] Energy Research Institute @ NTU, Nanyang Technological University, Singapore 637141, Singapore; weizb@ntu.edu.sg (Z. W.); lengfeng@ntu.edu.sg (F. L.); zjhe@ntu.edu.sg (Z. H.); zhang.wy@ntu.edu.sg (W. Z.); kyli@ntu.edu.sg (K. L.)

* Correspondence: weizb@ntu.edu.sg; Tel.: +65-83488230

Abstract: The accurate monitoring of state of charge (SOC) and state of health (SOH) is critical for the reliable management of lithium-ion battery (LIB) systems. In this paper, the online model identification is scrutinized to achieve high modeling accuracy and robustness, and a model-based joint estimator is further proposed to estimate the SOC and SOH of LIB concurrently. Specifically, an adaptive forgetting recursive least squares (AF-RLS) method is exploited to optimize the estimation alertness and numerical stability, so as to achieve accurate online adaption of model parameters. Leveraging the online adapted battery model, a joint estimator is proposed by combining an open-circuit voltage (OCV) observer with a low-order state observer to co-estimate the SOC and capacity of LIB. Simulation and experimental studies are performed to evaluate the performance of the proposed data-model fusion method. Results suggest that the proposed method can effectively track the variation of model parameters by using the onboard measured current and voltage data. The SOC and capacity can be further estimated in real time with fast convergence, high accuracy and high stability.

Keywords: state of charge; state of health; model identification; estimation; lithium-ion battery.

---

1. Introduction

Lithium-ion battery (LIB) is one of the leading energy storage technologies and has been widely applied in many fields like modern electric grids, portable electronics, and transportation electrification [1, 2]. To date, lots of efforts have been made to the improvement of cell chemistry, material and component. However, LIBs are typically complicated in the electrochemical perspective and the performance is easily degraded in the long-term operation. To this end, a high-fidelity battery management system (BMS) that accurately monitors the key battery states is critical for the safety, efficiency and life expectancy of LIB systems.

The state of charge (SOC) is the most important variable to be monitored in BMS. The accurate monitoring of SOC contributes to preventing the unsuitable over-charge or over-discharge which causes irreversible damage to LIB. The coulomb counting (CC) method is most widely used for commercial BMS products due to its simplicity and low computing cost. However, CC method is vulnerable to the current measurement error and depends on an accurate knowledge about the initial SOC, which problematize its application. The open-circuit voltage (OCV) measurement method is straightforward but needs a long relaxation time to obtain the accurate OCV, which is unrealistic in the continuous and dynamic load conditions.

The model-based observers enjoy the merits of high accuracy and robustness, thus have been widely studied for online SOC estimation in the literature [3]. An accurate battery serves as the prerequisite of this category of methods. In terms of LIB, existing models include the

© 2018 by the author(s). Distributed under a Creative Commons CC BY license.

Preprints (www.preprints.org) | NOT PEER-REVIEWED | Posted: 22 June 2018 doi:10.20944/preprints201806.0346.v1

Peer-reviewed version available at Energies 2018, 11, 1810; doi:10.3390/en11071810

electrochemical model [4-7], black-box model [8-10], and equivalent circuit model (ECM) [11, 12]. Amongst others, the ECMs have better trade-off between the model accuracy and complexity and thus are favorable candidates for the real-time application in micro-controller units. Generally, the dynamic behavior of LIB is simulated with ECMs, while the battery states are online estimated with a variety of observers, such as the Luenberger observer [13], extended Kalman filter (EKF) [14-16], square root cubature Kalman filter [17], unscented Kalman filter (UKF) [18, 19], sliding mode observer (SMO) [20], particle filter (PF) [21], nonlinear observer [22], etc. For these methods, the ECMs are calibrated offline and the model parameters are assumed to be fixed during the operation. Nevertheless, the model parameters of ECMs are typically affected by many factors, such as temperature, C-rate, SOC, and battery ageing status [23]. The lack of model adaption may decline the model robustness and estimation accuracy largely as the LIB systems are commonly operated under highly dynamic working conditions in real applications. In light of this, the integrated model identification and state estimation has been investigated to improve the overall robustness in recent years.

The existing co-estimation methods can be broadly categorized into three groups. The first group is called joint estimation which lumps the OCV and model parameters in one state vector for joint estimation with advanced filters, such as recursive least squares (RLS) [24] and KF-based methods [25]. The SOC is then inferred from the pre-calibrated SOC-OCV look-up table. The joint estimation methods manifest themselves with one filter to extract all the variables of interests, but the stability is a major challenge if model uncertainties are significant. The second group is called dual estimation which use two parallel filters to observer the model parameters and battery states concurrently [26]. For example, Xiong et al. [27] proposed a multi-scale dual extended Kalman filter (DEKF) to track the slow-varying model parameters and the fast dynamics of SOC accurately. Recently, the dual estimation method with different filtering techniques, i.e. EKF-based model identification and PF-based state estimation, was proposed for LIB management [28]. The third group is the data-model fusion method, which online identifies the model parameters with data-driven methods such as RLS, while simultaneously estimates the SOC with advanced filters [15, 29-31]. In recent years some modified methods like the vector-type RLS [32] was proposed to improve the performance of model parameters identification. This method is theoretically computationally efficient compared to the dual and joint estimation methods due to the low computing cost of RLS. For all the three groups of methods, the model robustness and estimation accuracy can be well improved, but the careful tuning is required to guarantee the algorithmic convergence and numerical stability. Also, the computing complexity may potentially barrier their application in low-cost micro-controllers, especially if using high-order models or observing multiple battery states. To this end, necessary modification will be of value to further improve the performance of estimation. Moreover, the instantaneous capacity is involved in the state-space formula of the model-based observers, thus the online update of it is critical to ensure a sufficient SOC accuracy over a long term operation.

The capacity is a direct indicator describing the state of health (SOH) of LIB. In the literature, the SOC and capacity were estimated concurrently with DEKF [33] and dual nonlinear predictive filter (DNPF) [34]. However, the model parameters are not fully adapted thus the robustness to dynamic working condition and ageing can be further improved. Alternatively, the capacity was lumped to the parameter vector, afterwards the model parameters and SOC were estimated simultaneously with DEKF [26, 35] to guarantee a high robustness. However, the dual and high-order EKF framework may suffer from instability issues and high computing cost which should be carefully addressed in real applications [36]. In Ref. [36], a multi-timescale estimator was proposed with the SOC estimated by a second-order EKF in micro timescale while the model parameters updated by an offline fourth-order EKF in the macro timescale. In Ref. [37], multiple proportional-integral estimators are formulated based on an electrochemical model to realize the concurrent estimation of impedance, SOC and capacity.

Although lots of efforts have been made towards the online estimation of SOC and SOH, major challenges still exist to improve the robustness and stability while lower down the computing cost.

Preprints (www.preprints.org) | NOT PEER-REVIEWED | Posted: 22 June 2018 doi:10.20944/preprints201806.0346.v1

Peer-reviewed version available at Energies 2018, 11, 1810; doi:10.3390/en11071810

In this paper, a new data-model fusion method is proposed to observe the SOC and SOH of LIB simultaneously based on an online adaptive battery model. The first-order RC model is adopted with the model parameters online identified with an adaptive forgetting recursive least squares (AF-RLS) method to enhance the tracking ability and numerical stability. Leveraging the online parameterized model, a joint estimator based on OCV pre-estimation and a low-order state observer is proposed to co-estimate the SOC and capacity, with the expectation to guarantee the stability and reduce the filtering dimension. Simulation and lab-scale experiments are further performed to verify the feasibility of the proposed method.

The rest of paper is organized as follows. The battery modeling and AF-RLS-based model identification are detailed in Section 2. The co-estimation of SOC and capacity with a simple OCV observer and HIF is put forward in Section 3. Section 4 and 5 present the simulation and experimental results to verify the proposed method. The main conclusions are drawn in Section 6.

2. Battery Modeling and Identification

2.1 Battery Modeling

An ECM with higher order can better reproduce the LIB dynamics with multiple time constants, but the higher computing complexity is not favorable for online embedded systems. Hu et al. [11] systematically studied the ECMs used for LIBs and found the first-order RC model kept a good trade-off between the model precision and computing complexity. The first-order RC model as shown in Figure 1 is thereby adopted in this paper to simulate the dynamics of LIB in use. The voltage source is used to simulate the OCV which is SOC-dependent. R_s is the ohmic resistance. The polarization resistance (R_p) and capacitance (C_p) construct a RC network to simulate the transient dynamics of LIB.

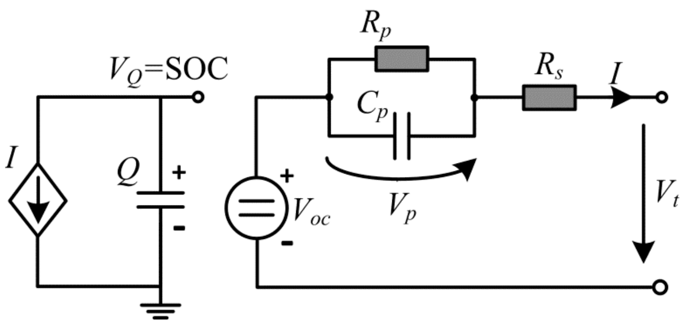

Figure 1. Circuit diagram of the first-order RC model.

The following governing equations can be written to describe the electrical behavior of the first-order RC model in use:

$$C_p \frac{dV_p}{dt} + \frac{V_p}{R_p} = I \tag{1}$$

$$V_t = V_{oc} - V_p - IR_s \tag{2}$$

where I is the load current which is defined as positive for discharge process throughout this paper, V_p and V_t are the polarization and terminal voltages, respectively. The OCV is a nonlinear function with respect to SOC. In this paper, the SOC-OCV function is determined by polynomial fitting to the offline tested SOC-OCV correction as:

$$V_{oc} = f(z) = \sum_{i=0}^{n_p} c_i z^i \tag{3}$$

where z is the battery SOC, n_p is the order of polynomial fitting (n_p = 5 in this paper), c_i is the polynomial coefficient obtained by the least squares-based curve fitting. The measured and curve-fitted SOC-OCV relations are shown in Figure 2.

Preprints (www.preprints.org) | NOT PEER-REVIEWED | Posted: 22 June 2018 doi:10.20944/preprints201806.0346.v1

Peer-reviewed version available at Energies 2018, 11, 1810; doi:10.3390/en11071810

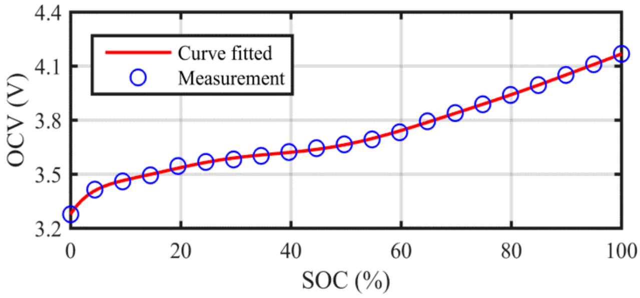

Figure 2. Measured and calibrated correlation between the SOC and OCV.

2.2 Online Identification of Model Parameters

This paper identifies the model parameters by formulating a regression problem. A new variable is defined as $y = V_t - V_{oc}$, then the transfer function of Eq. (1) can be expressed as:

$$\frac{y(s)}{I(s)} = -\frac{R_s + R_p + R_s R_p C_p s}{1 + R_p C_p s} \tag{4}$$

By adopting the bilinear transform $s = 2\,(q-1)\,/\,t_s\,/\,(q+1)$, Eq. (4) can be re-written as:

$$\frac{y(q^{-1})}{I(q^{-1})} = \frac{b_0 + b_1 q^{-1}}{1 + a_1 q^{-1}} \tag{5}$$

where

$$\begin{aligned} a_1 &= \frac{t_s - 2R_p C_p}{t_s + 2R_p C_p} \\ b_0 &= -\frac{R_s t_s + R_p t_s + 2R_s R_p C_p}{t_s + 2R_p C_p} \\ b_1 &= -\frac{R_s t_s + R_p t_s - 2R_s R_p C_p}{t_s + 2R_p C_p} \end{aligned} \tag{6}$$

where t_s is the onboard sampling interval. From Eq. (5), the following discrete-time expression can be written as:

$$y_k = \boldsymbol{\theta}_k^{\mathrm{T}} \boldsymbol{\varphi}_k \tag{7}$$

where $\boldsymbol{\theta}_k = [a_{1,k} \quad b_{0,k} \quad b_{1,k}]^{\mathrm{T}}$, $\boldsymbol{\varphi}_k = [-y_{k-1} \quad I_k \quad I_{k-1}]^{\mathrm{T}}$. Then the model identification problem boils down to solving the regression model represented by Eq. (7).

2.3 Adaptive Forgetting Recursive Least Squares

A classical method to solve Eq. (7) is the RLS method. The estimation law of RLS is given by:

Parameter vector update law:

$$\hat{\boldsymbol{\theta}}_k = \hat{\boldsymbol{\theta}}_{k-1} + \mathbf{L}_k \left(y_k - \hat{\boldsymbol{\theta}}_{k-1}^{\mathrm{T}} \boldsymbol{\varphi}_k \right) \tag{8}$$

Gain update law:

$$\mathbf{L}_k = \mathbf{P}_{k-1} \boldsymbol{\varphi}_k \left(\lambda + \boldsymbol{\varphi}_k^{\mathrm{T}} \mathbf{P}_{k-1} \boldsymbol{\varphi}_k \right)^{-1} \tag{9}$$

Covariance matrix update:

$$\mathbf{P}_k = \frac{1}{\lambda} \left(\mathbf{P}_{k-1} - \frac{\mathbf{P}_{k-1} \boldsymbol{\varphi}_k \boldsymbol{\varphi}_k^{\mathrm{T}} \mathbf{P}_{k-1}}{\lambda + \boldsymbol{\varphi}_k^{\mathrm{T}} \mathbf{P}_{k-1} \boldsymbol{\varphi}_k} \right) \tag{10}$$

The basic RLS assumes that λ = 1, which makes the covariance matrix decays gradually thus the algorithm cannot retain necessary alertness or adaptivity to track the time-varying parameters.

Peer-reviewed version available at Energies 2018, 11, 1810; doi:10.3390/en11071810

One simple method to ensure the estimation alertness is to use a forgetting factor of $\lambda < 1$, which means heavier weights are given to the more recent data. However, the selection of forgetting factor is an interesting trade-off that should be addressed carefully. Specifically, a small λ leads to large **P** and **L** thus the estimates tend to be uncertain. In contrast, a large λ potentially causes the loss of tracking capability for fast-varying parameters. This can be explained by analyzing Eq. (10): under sufficient excitation, the term on the right-hand side inside the square brackets decays faster than it is inflated by the multiplier $1/\lambda$, resulting in the gradual decay of covariance matrix.

Moreover, the exponential forgetting potentially leads the covariance wind-up problem under the low excitation condition. This is because the term $\mathbf{P}_{k-1}\boldsymbol{\varphi}_k$ in this case is close to zero, thus Eq. (10) becomes $\mathbf{P}_k = \mathbf{P}_k / \lambda$ indicating that the covariance matrix grows exponentially. When the excitation recovers, the covariance matrix and gain have been very large which cause large fluctuations on the estimation.

In seeking to overcome the aforementioned drawbacks of basic RLS and RLS with exponential forgetting, the use of adaptive forgetting factor is suggested by modifying Eqs. (9) and (10) according to [38]:

$$\mathbf{L}_k = \mathbf{P}_{k-1}\boldsymbol{\varphi}_k\left(1+\boldsymbol{\varphi}_k^{\mathrm{T}}\mathbf{P}_{k-1}\boldsymbol{\varphi}_k\right)^{-1} \tag{11}$$

$$\lambda_k = 1-\frac{\varepsilon_k^2}{\sigma\left(1+\boldsymbol{\varphi}_k^{\mathrm{T}}\mathbf{P}_{k-1}\boldsymbol{\varphi}_k\right)} \tag{12}$$

$$\mathbf{W}_k = \left(\mathbf{I}-\mathbf{L}_k\boldsymbol{\varphi}_k^{\mathrm{T}}\right)\mathbf{P}_{k-1} \tag{13}$$

where ε is the estimation residual calculated by:

$$\varepsilon_k = y_k - \boldsymbol{\varphi}_k^{\mathrm{T}}\hat{\boldsymbol{\theta}}_{k-1} \tag{14}$$

To impose an upper bound on the covariance matrix, **P** is updated as [39]:

$$\mathbf{P}_k = \begin{cases} \mathbf{W}_k/\lambda_k, & \text{trace }(\mathbf{W}_k/\lambda) \le C \\ \mathbf{W}_k, & \text{otherwise} \end{cases} \tag{15}$$

The above update laws comprise the AF-RLS which will be used in this paper for the online identification of model parameters. It is clear that the forgetting factor is online adaptive, with λ automatically set close to 1 when the estimation residual is small while set to a small value when the estimation residual is large. It should be noted two more tuning parameters have been introduced by the adaption of forgetting factor, i.e. the gain (σ) controlling the sensitivity of forgetting factor to the output mismatch and the upper bound to the trace of covariance matrix (C).

3. Co-estimation of SOC and SOH

Based on the online adaptive model described in Section 2, this section further seeks to propose a low-order estimator to estimate the SOC and SOH jointly. The capacity is used as the indicator for SOH in this paper.

3.1. H-infinity Filter

Compared with the well-known Kalman filtering (KF) based methods, the HIF can better withstand the modelling uncertainty and the estimation accuracy is not dependent on the knowledge of noise statistics. It is thereby expected that the estimation will have a better robustness to the model uncertainty and noise statistics [40]. A general nonlinear discrete-time state-space equation is expressed as:

Peer-reviewed version available at Energies 2018, 11, 1810; doi:10.3390/en11071810

$$\begin{aligned}\mathbf{x}_{k+1} &= F(\mathbf{x}_k, \mathbf{u}_k) + \mathbf{w}_k \\ y_k &= G(\mathbf{x}_k, \mathbf{u}_k) + v_k \\ \boldsymbol{\delta}_k &= \mathbf{h}_k \mathbf{x}_k \\ \mathbf{w}_k &\sim (0, \mathbf{Q}), v_k \sim (0, R)\end{aligned} \tag{16}$$

where $\mathbf{x}_k$, $\mathbf{u}_k$ and y_k are the system state, input and measurement, respectively; $\mathbf{w}_k$ and v_k are respectively the process and measurement noises with covariance matrices $\mathbf{Q}$ and R; $\boldsymbol{\delta}_k$ is a linear combination of different system states while $\mathbf{h}_k$ is a user-defined matrix. The state-space model represented by Eq. (16) aims to obtain the optimized estimate of $\boldsymbol{\delta}_k$. It is needed to set $\mathbf{h}_k = \mathbf{I}$ if $\mathbf{x}_k$ is estimated directly. The solution of HIF can be boiled down to minimize the following cost function:

$$\Im = \frac{\sum_{k=0}^{N-1} \left\| \boldsymbol{\delta}_k - \hat{\boldsymbol{\delta}}_k \right\|_{\mathbf{S}_k}^2}{\left\| \mathbf{x}_0 - \hat{\mathbf{x}}_0 \right\|_{\mathbf{P}_0^{-1}}^2 + \sum_{k=0}^{N-1} \left(\left\| \mathbf{w}_k \right\|_{\mathbf{Q}_k^{-1}}^2 + \left\| v_k \right\|_{R_k^{-1}}^2 \right)} \tag{17}$$

where $\mathbf{S}_k$ and $\mathbf{P}_0$ are user-defined symmetric positive matrices. To ease solving the optimization problem defined by Eq. (17), a performance bound (τ) is defined to arrive at an optimal estimation strategy which ensures that the cost function is smaller than $1/\tau$. The general procedures to implement the HIF are summarized in Table 1.

Table 1. Algorithmic procedures of HIF

Definition: $\hat{\mathbf{A}}_k = \left.\frac{\partial F}{\partial \mathbf{x}}\right\|_{\mathbf{x}_k = \hat{\mathbf{x}}_k^+}, \hat{\mathbf{C}}_k = \left.\frac{\partial G}{\partial \mathbf{x}}\right\|_{\mathbf{x}_k = \hat{\mathbf{x}}_k^+}$	
Initialization: $\hat{\mathbf{x}}_0^+$, $\mathbf{P}_0^+$, $\mathbf{Q}$, R, $\mathbf{S}_0$, τ	
For k**=1, 2, …**	
Update of priori state:	$\hat{\mathbf{x}}_k^- = F(\hat{\mathbf{x}}_{k-1}^+, \mathbf{u}_{k-1})$
Update of priori error covariance:	$\mathbf{P}_k^- = \hat{\mathbf{A}}_{k-1} \mathbf{P}_{k-1}^+ \hat{\mathbf{A}}_{k-1}^T + \mathbf{Q}$
Update of symmetric positive matrix:	$\mathbf{M}_k = \mathbf{h}_k^{\mathrm{T}} \mathbf{S}_k \mathbf{h}_k$
Update of gain matrix:	$\mathbf{K}_k = \hat{\mathbf{A}}_k \mathbf{P}_k^- \left(\mathbf{I} - \tau \mathbf{M}_k \mathbf{P}_k^- + \hat{\mathbf{C}}_k^{\mathrm{T}} R_k^{-1} \hat{\mathbf{C}}_k \mathbf{P}_k^- \right)^{-1} \hat{\mathbf{C}}_k^{\mathrm{T}} R_k^{-1}$
Update of posteriori state:	$\hat{\mathbf{x}}_k^+ = \hat{\mathbf{x}}_k^- + \mathbf{K}_k \left[y_k - G(\hat{\mathbf{x}}_k^-, \mathbf{u}_k) \right]$
Update of posteriori error covariance:	$\mathbf{P}_k^+ = \mathbf{P}_k^- \left(\mathbf{I} - \tau \mathbf{M}_k \mathbf{P}_k^- + \hat{\mathbf{C}}_k^{\mathrm{T}} R_k^{-1} \hat{\mathbf{C}}_k \mathbf{P}_k^- \right)^{-1}$

3.2. OCV Observation

With the HIF detailed in Section 3.1, the SOC and capacity can be observed in real time by using the procedures summarized in Table 1.

The existing state observers typically lump multiple system states including the polarization voltages and the LIB states of interests into one vector for observation. A potential problem is that the filtering with high order is prone to high computing cost and low stability due to the high-dimension matrix operation and the cross interferences among multiple system states. In light of this, order reduction is always plausible for the accurate state estimation. This paper thus also seeks to propose a low-order state observer for SOC and SOH joint estimation. To realize this, a simple OCV observer is first proposed. It is clear that Eq. (7) can be rewritten in the discrete-time domain as:

$$V_{t,k} - V_{oc,k} = -a_1 \left(V_{t,k-1} - V_{oc,k-1} \right) + b_0 I_k + b_1 I_{k-1} \tag{18}$$

Adopting transposition to Eq. (18) yields:

$$V_{oc,k} = \hat{V}_{oc,k} + \Delta_k \tag{19}$$

where $\hat{V}_{oc,k}$ and Δ_k are the OCV estimate and the estimation residual, which can be expressed as:

Preprints (www.preprints.org) | NOT PEER-REVIEWED | Posted: 22 June 2018 doi:10.20944/preprints201806.0346.v1

Peer-reviewed version available at *Energies* **2018**, *11*, 1810; doi:10.3390/en11071810

$$\begin{aligned} \hat{V}_{oc,k} &= \frac{V_{t,k} + a_1 V_{t,k-1} - b_0 I_k - b_1 I_{k-1}}{1 + a_1} \\ \Delta_k &= \frac{a_1}{1 + a_1}\left(V_{oc,k} - V_{oc,k-1}\right) \end{aligned} \tag{20}$$

It is shown that the estimation residual is close to zero if the OCV changes slowly during two adjacent sampling times. The $\hat{V}_{oc,k}$ can thereby be viewed as the OCV estimate with small disturbances. The deduction in this subsection is a general framework thus can be easily extended to fit to higher-order RC models.

3.3. Joint Estimaiton of SOC and Capacity

The capacity is used to infer the SOH of LIB. A close-loop observer is formulated here by using the online adapted ECM to online estimate the SOC and capacity concurrently. The state-space model in the form of Eq. (16) should be formulated firstly to allow the use of HIF in Table 1.

As a major difference from the existing joint estimators, in this paper, the $\hat{V}_{oc}$ in Eq. (19) is viewed as the noisy system measurement. In this regard, the polarization voltage (V_p) can be ruled out from the state vector as it has no correlation with the OCV. Therefore, the state vector is defined as $\mathbf{x} = [z, 1/Q]^{\mathrm{T}}$, while the system input and output are defined as I and $\hat{V}_{oc}$, respectively. The following state-space formula can then be formulated:

$$\begin{aligned} \mathbf{x}_{k+1} &= F\left(\mathbf{x}_k, \mathbf{u}_k\right) + \mathbf{w}_k = \begin{bmatrix} 1 & -\eta t_s I_k \\ 0 & 1 \end{bmatrix} \mathbf{x}_k + \mathbf{w}_k \\ \hat{V}_{oc} &= G\left(\mathbf{x}_k, \mathbf{u}_k\right) + v_k \end{aligned} \tag{21}$$

where $G(\mathbf{x}_k, \mathbf{u}_k)$ is the function of OCV with regard to the system state and input, which can be determined by the calibrated SOC-OCV function expressed by Eq. (3).

Referring to the state-space formula expressed by Eq. (21), the reference matrices ($\hat{\mathbf{A}}_k$ and $\hat{\mathbf{C}}_k$) in Table 1 can be expressed as:

$$\begin{aligned} \hat{\mathbf{A}}_k &= \left.\frac{\partial F}{\partial \mathbf{x}}\right|_{\mathbf{x}_k = \hat{\mathbf{x}}_k^+} = \begin{bmatrix} 1 & -\eta t_s I_k \\ 0 & 1 \end{bmatrix} \\ \hat{\mathbf{C}}_k &= \left.\frac{\partial G}{\partial \mathbf{x}}\right|_{\mathbf{x}_k = \hat{\mathbf{x}}_k^+} = \begin{bmatrix} \left.\dfrac{dV_{oc}}{dz}\right|_{z_k = \hat{z}_k} & 0 \end{bmatrix} \end{aligned} \tag{22}$$

The HIF can then be used to keep tracking of both the SOC and capacity leveraging the described definitions and algorithmic procedures. As the polarization voltage has been ruled out from the state vector, the dimension of filtering is effectively reduced. It has to be pointed out that the dimension compression will be more significant based on the proposed method if models with higher orders are in use.

4. Simulation Study

This section aims to verify the feasibility of the proposed method on both online model identification and state joint estimation with simulations. An ideal battery model is used to eliminate the modeling uncertainties, so that the method can be well evaluated from the pure theoretical prospective.

4.1. Data Acquisition

The first-order ECM as shown in Figure 1 was built in Matlab/Simulink Environment. The OCV was defined with the calibrated SOC-OCV function of the cell in use. The ohmic resistance

Preprints (www.preprints.org) | NOT PEER-REVIEWED | Posted: 22 June 2018 doi:10.20944/preprints201806.0346.v1

Peer-reviewed version available at Energies 2018, 11, 1810; doi:10.3390/en11071810

and polarization resistance were defined to be time-variant, while the polarization capacitance was assumed to be constant at a user-defined value. A user-defined hybrid pulse test (HPT) and the Federal Urban Dynamic Schedule (FUDS) were used in this section to test the performance of the proposed method. The current profiles were loaded to the ECM in Simulink and the corresponding terminal voltage and SOC were obtained accordingly. The current and voltage data of the two simulations are shown in Figure 3.

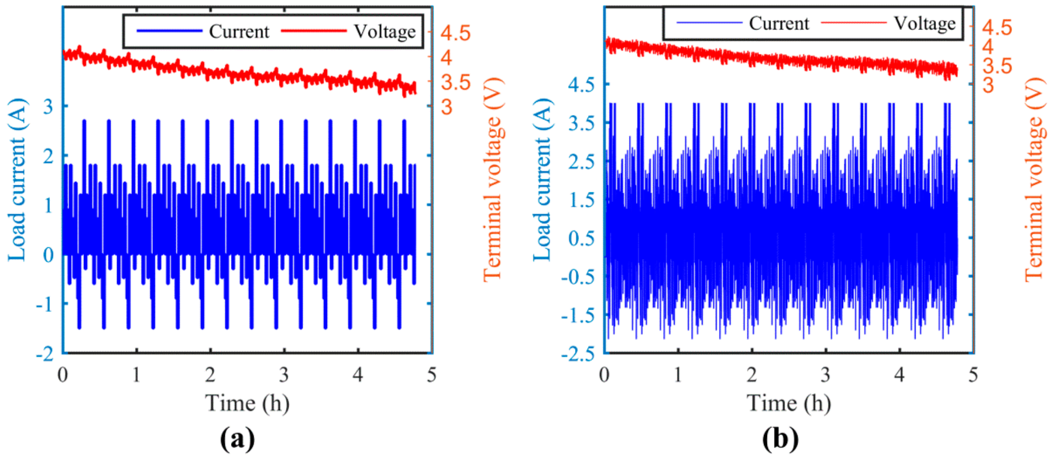

Figure 3. Load current and terminal voltage of simulation study: (a) HPT; (b) FUDS.

4.2. Simulation Results

The simulated current and voltage data are used to verify the proposed method. As no prior knowledge can be obtained on the model parameters and system states, the algorithm is randomly initialized as follows throughout this paper of not otherwise defined: $R_s = R_p = 10$ mΩ, $C_p = 1$ kF, $SOC_0 = 60\%$, $Q_0 = 1.8$ Ah.

The results of online model identification under the HPT condition are shown in Figure 4. It is shown that the proposed method can track the change of all parameters effectively. The identification experiences a short transition time with certain overshooting for the correction of erroneous initialization at the initial stage, and afterwards the model parameters have been identified with reasonable accuracy. The online adaption of model parameters facilitates keeping a high modelling accuracy and a good robustness for state estimation.

The results of SOC and capacity joint estimation under the HPT are shown in Figure 5. As shown, the proposed method keeps tracking of the reference SOC accurately with rapid convergence from the large initialization error of 35%. The estimation error has been well confined to 1% error bound for the entire simulation. The capacity estimation is also shown to converge to the expected value. However, the convergence is much slower compared to the estimation of SOC. This is because the capacity changes very slowly in real applications, so that a very small process noise covariance component is assigned to the capacity-relevant state to stabilize the estimation. It can be observed that the estimated capacity matches closely with the reference value once the algorithm converges.

Preprints (www.preprints.org) | NOT PEER-REVIEWED | Posted: 22 June 2018 doi:10.20944/preprints201806.0346.v1

Peer-reviewed version available at Energies 2018, 11, 1810; doi:10.3390/en11071810

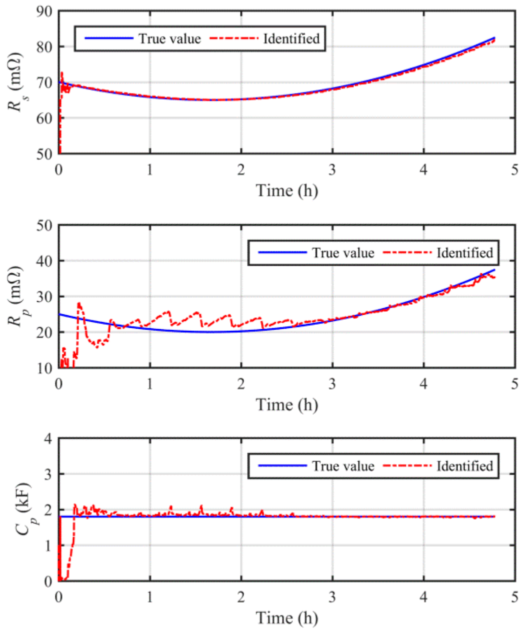

Figure 4. Results of online model parameters identification under the HPT of simulation study.

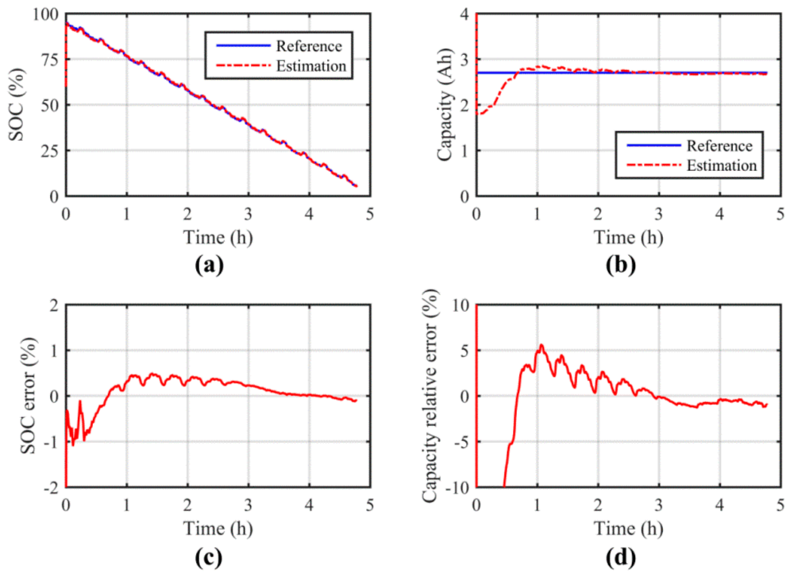

Figure 5. Results of SOC and capacity joint estimation under the HPT of simulation study: (a) estimation of SOC; (b) estimation of capacity; (c) error of SOC estimation; (d) relative error of capacity estimation.

Results of online model identification and state joint estimation under the FUDS condition are shown in Figure 6 and Figure 7, respectively. Similar to the case under HPT condition, the proposed method shows an easy convergence and a high accuracy on model identification, SOC and capacity estimation.

To give a quantitative evaluation for the algorithmic performance, the mean absolute error (MAE) and rooted mean square error (RMSE) of SOC estimation as important performance measures are summarized in Table 2, while the mean relative error (MRE) and RMSE of capacity estimation are summarized in Table 3. It should be noted that all the performance measures are calculated after the estimation converges to the 10% error bound, in seeking to rule out the uncertain impact of the convergence process. Results suggest that the estimation is of high fidelity in terms of online estimation, thus the theoretical feasibility of the proposed method has been confirmed.

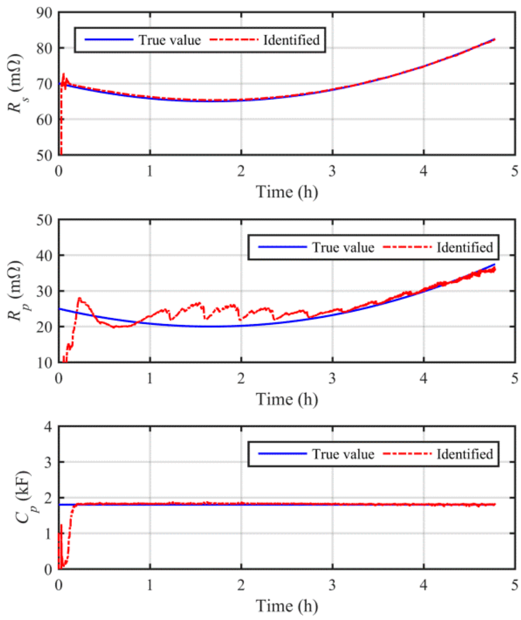

Figure 6. Results of online model parameters identification under the FUDS of simulation study.

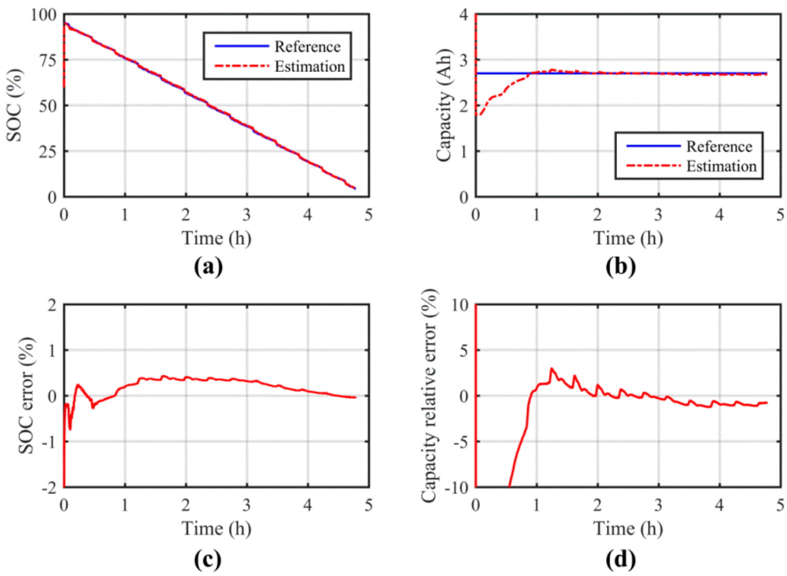

Figure 7. Estimation results of SOC and capacity under the FUDS of simulation study: (a) estimation of SOC; (b) estimation of capacity; (c) error of SOC estimation; (d) relative error of capacity estimation.

Table 2. Algorithmic performance on SOC estimation for the simulation study

Measure	HPT	FUDS
MAE	0.26%	0.23%
RMSE	0.33%	0.27%

Table 3. Algorithmic performance on capacity estimation for the simulation study

Measure	HPT	FUDS
MRE	1.70%	1.16%
RMSE	2.32%	1.95%

Preprints (www.preprints.org) | NOT PEER-REVIEWED | Posted: 22 June 2018 doi:10.20944/preprints201806.0346.v1

Peer-reviewed version available at Energies 2018, 11, 1810; doi:10.3390/en11071810

5. Experimental Study

The simulation study in Section 4 is based on an ideal ECM to evaluate the proposed method from the theoretical prospective. It should be noted that both the model identification and state estimation can be adversely impacted by modeling uncertainties, such as the fitting error of SOC-OCV correlation and the unmodeled battery dynamics. Therefore, the proposed method is further evaluated with lab-scale experiments in this section.

5.1. Experimental Setup

Experiments are performed on a Samsung 18650 lithium-ion battery which has a nominal capacity of 2200 mAh. The hybrid pulse current as shown in Figure 3 (a) is inputted to the LIB with a cell-level battery testing system, while the terminal voltage are collected accordingly. The current and voltage sensors have measurement ranges of 10 A and 5 V respectively, while the error limits of sensing are both within 0.05%. The ambient temperature is controlled at 22°C for all experiments. The data of interests are sampled at 1 Hz by using a data acquisition system and stored in a host computer.

5.2. Reference Data Extraction

The reference SOC profile is required to verify the result of SOC estimation. It is well known that the CC method can obtain the reference SOC accurately if the cell can be preset to a known SOC. To achieve this, the cell is fully charged under the CCCV mode and then discharged to the desired initial SOC by CC. The reference SOC can then be obtained for the entire experiment with the known initial SOC.

The verification of propose method on model identification results requires the reference values of model parameters. For this purpose, several time points are selected at a defined time interval during the HPT. Around each time point, a set of current and voltage signals are sampled, based on which the reference values of model parameters can be extracted offline. Specifically, R_s is calibrated by the instantaneous voltage jump following a step change of current, i.e. $R_s=\Delta V_t / \Delta I$. As OCVs can be known from the CC-based reference SOCs, R_p and C_p can be determined by fitting the voltage responses to real measurements.

5.3. Experimental Results

The experimental results of online model identification are shown in Figure 8. From the offline calibration results, it is shown that all the model parameters exhibit time-variant features which further confirm the necessity of online model adaption to keep a sufficient modeling accuracy. To this end, the existing observing techniques with fixed battery models are theoretically less accurate due to the lack of adaptability to the variation of working conditions. By using the proposed method, it is observed that the identification converges from the initialization error and tracks the varying model parameters with reasonable accuracy. The error-prone and time-consuming model calibration can thereby be avoided with the mechanism of online model adaption.

Based on the online adapted model parameters, the SOC and capacity are estimated jointly and shown in Figure 9. It is shown that the estimated SOC converges very fast from the large initialization offset, and afterwards the trajectory of reference SOC has been projected accurately with the error confined to 1% error bound throughout the experiment. By comparison, the estimated capacity also converges stably to the reference value, but the convergence is slower than the SOC estimation. Once the estimation converges, the capacity estimation error is well constrained within 5%. The performance measures including MAE and RMSE are summarized in Table 4 to give a quantitative evaluation. Compared to the simulation results in Table 2 and Table 3,

Preprints (www.preprints.org) | NOT PEER-REVIEWED | Posted: 22 June 2018 doi:10.20944/preprints201806.0346.v1

Peer-reviewed version available at Energies 2018, 11, 1810; doi:10.3390/en11071810

the accuracy is slightly lower but is still quite favorable in terms of online estimation. Is spite of the existence of model uncertainties in real experiments, the estimation proves to be highly accurate for both SOC and capacity.

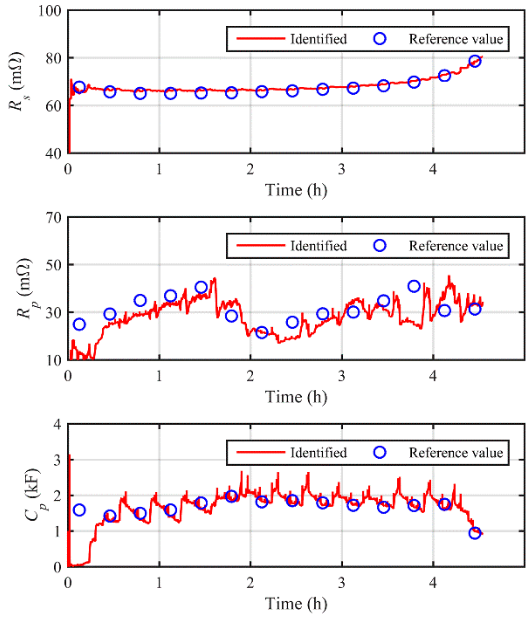

Figure 8. Results of online model parameters identification for experimental study.

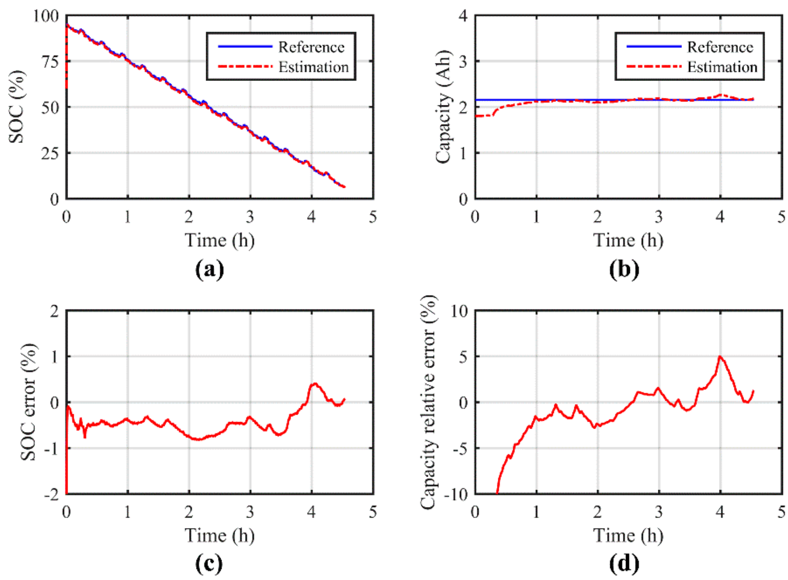

Figure 9. Estimation results of SOC and capacity for experimental study: (a) estimation of SOC; (b) estimation of capacity; (c) error of SOC estimation; (d) relative error of capacity estimation.

Table 4. Algorithmic performance on SOC and capacity estimation for the experimental study

Measure	SOC	Capacity
MAE	0.45%	0.045 Ah (MRE = 2.10%)
RMSE	0.46%	0.073 Ah (MRE = 3.38%)

6. Conclusions

This paper proposes a new data-model fusion method for SOC and SOH co-estimation based on an online adaptive battery model. The model parameters are online identified with the AF-RLS

Preprints (www.preprints.org) | NOT PEER-REVIEWED | Posted: 22 June 2018 doi:10.20944/preprints201806.0346.v1

Peer-reviewed version available at *Energies* **2018**, *11*, 1810; doi:10.3390/en11071810

method to keep high modeling accuracy and robustness. Based on the online adaptive model, a joint estimator based on OCV observation and a low-order state observer is proposed to achieve the co-estimation of SOC and capacity. Simulation and experimental results suggest that the proposed method can keep tracking of the model parameters effectively. The SOC and capacity estimation have also been verified with fast convergence, high accuracy and high stability. As a data-driven method, the proposed method online requires the onboard measured current and voltage data thus has a good prospect for real applications in BMSs.

Peer-reviewed version available at Energies 2018, 11, 1810; doi:10.3390/en11071810

Author Contributions: Methodology, Zhongbao Wei; Resources, Feng Leng and Zhongjie He; Validation, Zhongbao Wei, Wenyu Zhang and Kaiyuan Li; Writing – original draft, Zhongbao Wei; Writing – review & editing, Feng Leng, Zhongjie He, Wenyu Zhang and Kaiyuan Li.

Funding: This research received no external funding.

Conflicts of Interest: The authors declare no conflict of interest.

References

1. Hu, X.; Zou, C.; Zhang, C.; Li, Y., Technological developments in batteries: a survey of principal roles, types, and management needs. *IEEE Power and Energy Magazine* **2017,** 15, (5), 20-31.
2. Zhou, L.; Zheng, Y.; Ouyang, M.; Lu, L., A study on parameter variation effects on battery packs for electric vehicles. *Journal of Power Sources* **2017,** 364, 242-252.
3. Tang, X.; Liu, B.; Gao, F.; Lv, Z., State-of-charge estimation for li-ion power batteries based on a tuning free observer. *Energies* **2016,** 9, (9), 675.
4. Zheng, L.; Zhu, J.; Wang, G.; Lu, D. D. C.; He, T., Lithium-ion battery instantaneous available power prediction using surface lithium concentration of solid particles in a simplified electrochemical model. *IEEE Transactions on Power Electronics* **2018**, 1-1.
5. Zou, C.; Manzie, C.; Nešić, D.; Kallapur, A. G., Multi-time-scale observer design for state-of-charge and state-of-health of a lithium-ion battery. *Journal of Power Sources* **2016,** 335, 121-130.
6. Sturm, J.; Ennifar, H.; Erhard, S.; Rheinfeld, A.; Kosch, S.; Jossen, A., State estimation of lithium-ion cells using a physicochemical model based extended Kalman filter. *Applied Energy* **2018,** 223, 103-123.
7. Moura, S. J.; Argomedo, F. B.; Klein, R.; Mirtabatabaei, A.; Krstic, M., Battery State Estimation for a Single Particle Model With Electrolyte Dynamics. *IEEE Transactions on Control Systems Technology* **2017,** 25, (2), 453-468.
8. Meng, J.; Luo, G.; Gao, F., Lithium Polymer Battery State-of-Charge Estimation Based on Adaptive Unscented Kalman Filter and Support Vector Machine. *IEEE Transactions on Power Electronics* **2016,** 31, (3), 2226-2238.
9. Charkhgard, M.; Farrokhi, M., State-of-charge estimation for lithium-ion batteries using neural networks and EKF. *IEEE transactions on industrial electronics* **2010,** 57, (12), 4178-4187.
10. Tang, X.; Yao, K.; Liu, B.; Hu, W.; Gao, F., Long-Term Battery Voltage, Power, and Surface Temperature Prediction Using a Model-Based Extreme Learning Machine. *Energies* **2018,** 11, (1), 86.
11. Hu, X.; Li, S.; Peng, H., A comparative study of equivalent circuit models for Li-ion batteries. *Journal of Power Sources* **2012,** 198, 359-367.
12. Kim, T.; Wang, Y.; Fang, H.; Sahinoglu, Z.; Wada, T.; Hara, S.; Qiao, W., Model-based condition monitoring for lithium-ion batteries. *Journal of Power Sources* **2015,** 295, 16-27.
13. Wei, Z.; Meng, S.; Xiong, B.; Ji, D.; Tseng, K. J., Enhanced online model identification and state of charge estimation for lithium-ion battery with a FBCRLS based observer. *Applied Energy* **2016,** 181, 332-341.
14. Plett, G. L., Extended Kalman filtering for battery management systems of LiPB-based HEV battery packs: Part 3. State and parameter estimation. *Journal of Power Sources* **2004,** 134, (2), 277-292.
15. Wang, Y.; Zhang, X.; Liu, C.; Pan, R.; Chen, Z., Multi-timescale power and energy assessment of lithium-ion battery and supercapacitor hybrid system using extended Kalman filter. *Journal of Power Sources* **2018,** 389, 93-105.
16. Wei, Z.; Bhattarai, A.; Zou, C.; Meng, S.; Lim, T. M.; Skyllas-Kazacos, M., Real-time monitoring of capacity loss for vanadium redox flow battery. *Journal of Power Sources* **2018,** 390, 261-269.

Preprints (www.preprints.org) | NOT PEER-REVIEWED | Posted: 22 June 2018 doi:10.20944/preprints201806.0346.v1

Peer-reviewed version available at Energies 2018, 11, 1810; doi:10.3390/en11071810

17. Cui, X.; Jing, Z.; Luo, M.; Guo, Y.; Qiao, H., A New Method for State of Charge Estimation of Lithium-Ion Batteries Using Square Root Cubature Kalman Filter. *Energies* **2018,** 11, (1), 209.
18. Dong, G.; Wei, J.; Chen, Z.; Sun, H.; Yu, X., Remaining dischargeable time prediction for lithium-ion batteries using unscented Kalman filter. *Journal of Power Sources* **2017,** 364, 316-327.
19. Chen, Y.; Huang, D.; Zhu, Q.; Liu, W.; Liu, C.; Xiong, N., A New State of Charge Estimation Algorithm for Lithium-Ion Batteries Based on the Fractional Unscented Kalman Filter. *Energies* **2017,** 10, (9), 1313.
20. Huangfu, Y.; Xu, J.; Zhao, D.; Liu, Y.; Gao, F., A Novel Battery State of Charge Estimation Method Based on a Super-Twisting Sliding Mode Observer. *Energies* **2018,** 11, (5), 1-21.
21. Wang, Y.; Zhang, C.; Chen, Z., A method for state-of-charge estimation of LiFePO4 batteries at dynamic currents and temperatures using particle filter. *Journal of Power Sources* **2015,** 279, 306-311.
22. Zhao, L.; Ji, G.; Liu, Z., Design and Experiment of Nonlinear Observer with Adaptive Gains for Battery State of Charge Estimation. *Energies* **2017,** 10, (12), 2046.
23. Waag, W.; Fleischer, C.; Sauer, D. U., Critical review of the methods for monitoring of lithium-ion batteries in electric and hybrid vehicles. *Journal of Power Sources* **2014,** 258, 321-339.
24. Duong, V.-H.; Bastawrous, H. A.; Lim, K.; See, K. W.; Zhang, P.; Dou, S. X., Online state of charge and model parameters estimation of the LiFePO4 battery in electric vehicles using multiple adaptive forgetting factors recursive least-squares. *Journal of Power Sources* **2015,** 296, 215-224.
25. Xiong, R.; He, H.; Sun, F.; Zhao, K., Evaluation on state of charge estimation of batteries with adaptive extended Kalman filter by experiment approach. *IEEE Transactions on Vehicular Technology* **2013,** 62, (1), 108-117.
26. Hu, C.; Youn, B. D.; Chung, J., A multiscale framework with extended Kalman filter for lithium-ion battery SOC and capacity estimation. *Applied Energy* **2012,** 92, 694-704.
27. Xiong, R.; Sun, F.; Chen, Z.; He, H., A data-driven multi-scale extended Kalman filtering based parameter and state estimation approach of lithium-ion olymer battery in electric vehicles. *Applied Energy* **2014,** 113, (0), 463-476.
28. Dong, G.; Chen, Z.; Wei, J.; Zhang, C.; Wang, P., An online model-based method for state of energy estimation of lithium-ion batteries using dual filters. *Journal of Power Sources* **2016,** 301, 277-286.
29. Xiong, R.; Sun, F.; Gong, X.; Gao, C., A data-driven based adaptive state of charge estimator of lithium-ion polymer battery used in electric vehicles. *Applied Energy* **2014,** 113, 1421-1433.
30. Wei, J.; Dong, G.; Chen, Z., On-board adaptive model for state of charge estimation of lithium-ion batteries based on Kalman filter with proportional integral-based error adjustment. *Journal of Power Sources* **2017,** 365, 308-319.
31. Zhang, Y.; Xiong, R.; He, H.; Shen, W., Lithium-Ion Battery Pack State of Charge and State of Energy Estimation Algorithms Using a Hardware-in-the-Loop Validation. *IEEE Transactions on Power Electronics* **2017,** 32, (6), 4421-4431.
32. Wei, Z.; Zhao, J.; Ji, D.; Tseng, K. J., A multi-timescale estimator for battery state of charge and capacity dual estimation based on an online identified model. *Applied Energy* **2017,** 204, 1264-1274.
33. Lee, S.; Kim, J.; Lee, J.; Cho, B. H., State-of-charge and capacity estimation of lithium-ion battery using a new open-circuit voltage versus state-of-charge. *Journal of power sources* **2008,** 185, (2), 1367-1373.
34. Hua, Y.; Cordoba-Arenas, A.; Warner, N.; Rizzoni, G., A multi time-scale state-of-charge and state-of-health estimation framework using nonlinear predictive filter for lithium-ion battery pack with passive balance control. *Journal of Power Sources* **2015,** 280, 293-312.

Preprints (www.preprints.org) | NOT PEER-REVIEWED | Posted: 22 June 2018 doi:10.20944/preprints201806.0346.v1

Peer-reviewed version available at *Energies* **2018**, *11*, 1810; doi:10.3390/en11071810

35. Xiong, R.; Sun, F.; Chen, Z.; He, H., A data-driven multi-scale extended Kalman filtering based parameter and state estimation approach of lithium-ion olymer battery in electric vehicles. *Applied Energy* **2014,** 113, 463-476.
36. Zou, Y.; Hu, X.; Ma, H.; Li, S. E., Combined state of charge and state of health estimation over lithium-ion battery cell cycle lifespan for electric vehicles. *Journal of Power Sources* **2015,** 273, 793-803.
37. Zheng, L.; Zhang, L.; Zhu, J.; Wang, G.; Jiang, J., Co-estimation of state-of-charge, capacity and resistance for lithium-ion batteries based on a high-fidelity electrochemical model. *Applied Energy* **2016,** 180, 424-434.
38. Fortescue, T.; Kershenbaum, L. S.; Ydstie, B. E., Implementation of self-tuning regulators with variable forgetting factors. *Automatica* **1981,** 17, (6), 831-835.
39. Cordero, A. O.; Mayne, D. In *Deterministic convergence of a self-tuning regulator with variable forgetting factor*, IEE Proceedings D-Control Theory and Applications, 1981; IET: 1981; pp 19-23.
40. Xia, B.; Zhang, Z.; Lao, Z.; Wang, W.; Sun, W.; Lai, Y.; Wang, M., Strong Tracking of a H-Infinity Filter in Lithium-Ion Battery State of Charge Estimation. *Energies* **2018,** 11, (6), 1-20.